Scaling behavior at the insulator-metal transition in $Bi_2Sr_2(Ca_zR_{1-z})Cu_2O_{8+y}$ where R is a rare-earth element

C. Quitmann, D. Andrich, C. Jarchow, M. Fleuster, B. Beschoten, and G. Güntherodt
2. Physikalisches Institut, Rheinisch-Westfälische Technische Hochschule Aachen, W-5100 Aachen, Germany

V. V. Moshchalkov*
Laboratory of High-T_c Superconductivity, Department of Physics, Moscow State University, Moscow 119899, Russia

G. Mante and R. Manzke
Institut für Experimentalphysik, Universität Kiel, W-2300 Kiel, Germany
(Received 6 April 1992; revised manuscript received 20 July 1992)

We report on the details of the insulator-metal transition (IMT) induced in $Bi_2Sr_2(Ca_z,R_{1-z})Cu_2O_{8+y}$ (R=Y, Gd, Nd) by Ca^{2+} doping. The resistivity in the insulating regime is analyzed using a generalized hopping approach based on the connectivity criterion. This enables us to estimate the dependence of the localization radius a_H on the Ca concentration independent of dimensionality. Insulating samples with a Y content not too far from the critical concentration $z_C=(0.43\pm0.02)$ show metallic conduction at high temperature and hopping conduction at low temperature. This shows the coexistence of delocalized and localized states separated by a disorder-induced mobility edge. Ultraviolet-photoemission-spectroscopy (UPS) spectra give evidence for both a shift in the Fermi level to lower energies and the development of new states at the Fermi level. The existence of a mobility edge together with the shift in E_F upon Ca^{2+} doping shows that the transition is probably of the Anderson type. We present a schematic picture for the density of states in the vicinity of E_F based on the results of spectroscopic and transport data. For this density of states we calculate the electrical resistivity using the Kubo-Greenwood formula. The results are in good qualitative agreement with the experiments. At the IMT the localization radius diverges and the metallic conductivity vanishes following a scaling law $\sigma=\sigma_0\{1-z/z_C\}^{\eta}$, with a critical exponent $\eta=1$ *A*.

I. INTRODUCTION

In oxide superconductors the metallic state and superconductivity can be easily suppressed by a proper variation of the chemical composition.[1-3] In the case of $Bi_2Sr_2CaCu_2O_{8+y}$ (Bi 2:2:1:2),[4] the metal-insulator transition may be realized by substitution of trivalent rare earth (R) for divalent Ca ions[5,6] and has been investigated by many authors using various different techniques.[7-16] In Bi 2:2:1:2 the metal-insulator transition can be introduced by substituting almost all rare-earth elements[7,8,14] and even Th (Ref. 17) for Ca.

While other authors have mostly focused on the composition range where the samples are superconducting, we will focus our attention on the insulating samples and scaling behavior of the conductivity at the insulator-metal transition (IMT). The $Bi_2Sr_2(Ca_z,R_{1-z})Cu_2O_{8+y}$ system is very well suited for studying the transition from a charge-transfer insulator (CTI) (Refs. 18 and 19) to a high-temperature superconductor (HTSC) because samples can be prepared which are reproducible and the results of different groups are in good agreement. In this paper we will use the insulating compound $Bi_2Sr_2YCu_2O_{8+y}$, which is the parent compound for the HTSC Bi 2:2:1:2 as a starting point for our discussion. This point of view is analogous to the $(La,Sr)_2CuO_{4-y}$ (Refs. 20 and 21) case where the insulator La_2CuO_4 is used as a starting point. Using this approach, the carrier concentration grows with the amount of doping z, similar to the case of traditional doped semiconductors.[22-25]

When studying insulator-metal transitions, samples are usually classified into two groups. Either they are insulators, meaning

$$\lim_{T\to 0,\omega\to 0}\rho(T,\omega)=\infty\ ,$$

or they are metals, meaning

$$\lim_{T\to 0,\omega\to 0}\rho(T,\omega)=\text{const}\ .$$

Metals show a linear resistivity $\rho\sim T$ at least in a limited region. In traditional metals such as the elements, this temperature dependence is well understood as originating from the scattering of free electrons by thermally excited Debye phonons. HTSC's also possess a linear resistivity, and this linear resistivity extends over a surprisingly large temperature interval.[2,26] However, the assumption of free electrons and Debye phonons is probably not valid in these compounds because of the strong correlations among the rather localized Cu 3*d* electrons.[19,27] Nevertheless, we will talk about a "metallic" resistivity in samples showing $\rho\sim T$, keeping in mind that its origin may be quite different. A possible origin for the observed linear resistivity will be discussed later in this paper.

II. EXPERIMENTAL DETAILS

A. Sample preparation and crystal structure

All experiments were performed on single-phase polycrystalline material. We have used polycrystalline material rather than single crystals because it is very difficult to grow homogeneous single crystals with controlled RE content in the region of low Ca content, which was most interesting to us. The samples were prepared by the standard procedure using oxides and carbonates as precursors. The preparation was identical for all samples except for the final sintering, which was carried out at 920 °C for samples with high Y content and at 865 °C for samples without Y. The higher sintering temperatures for samples with high Y content are necessary in order to avoid phase separation. The sintering was carried out in air, and samples were oven cooled to room temperature after sintering. The crystal structure was analyzed using powder x-ray diffraction. All reflexes could be assigned to the orthorhombic *Fmmm* space group.[28,29] The linewidths were almost independent of the Ca content [full width at half maximum (FWHM) $\leq 0.23°$ for the (00$\underline{10}$) peak], showing the homogeneous incorporation of the dopant. Upon doping, the *c* axis increases from 30.20 Å ($z=0$) to 30.81 Å ($z=1$). Both *a* and *b* axes decrease, and the orthorhombic splitting, which is 0.7% at $z=0$, becomes smaller and drops below our resolution at $z=0.7$.

B. Electrical resistivity and Hall effect

Electrical resistivity was measured by a four-probe ac technique using a constant-current source and a lock-in amplifier. The samples were bar shaped, and contacts were made by applying highly conductive silver paint. The absolute error in the resistivity data is dominated by the error in the sample geometry, which is approximately 5%. For Hall-effect measurements, we used a five-probe bridge technique to eliminate effects of the magnetoresistance. Samples were again bar shaped, and currents ranged between 10 and 50 mA. The measurements were performed in a superconducting solenoid with fields up to 6 T, and data were taken between T_c and room temperature. The Hall coefficient R_H was determined by using the derivative of the Hall voltage with respect to the magnetic field. During a field sweep, the temperature was kept stable to within 60 mK. The main error in R_H is the sample thickness, which is accurate to about 5%. Additional errors of about 3% come from noise pickup during the measurement because of the very weak signals ($\sim$ 500 nV).

C. Photoemission

The photoemission spectra were taken with He I radiation (21.22 eV) from a rare-gas discharge lamp. Photoelectrons were detected in normal emission with a hemispherical analyzer. The energy resolution was 130 meV for the valence-band spectra and 60 meV for the spectra near the Fermi level. The samples were attached to the sample holder by a conducting epoxy glue and cleaned *in situ* by scraping with a diamond file under ultra high-vacuum conditions just before the measurement. In order to avoid contamination of the surface during the measurement, the base pressure was kept in the low-10^{-10}-mbar range at all times. The Fermi edge of a gold film, which was evaporated *in situ* onto a separate sample holder prior to the measurements, was used as an energy reference. All spectra were taken at room temperature.

III. INSULATOR-METAL TRANSITION INDUCED BY CHEMICAL SUBSTITUTION

The composition and temperature dependence of the electrical resistivity shown in Fig. 1 most clearly shows the drastic changes introduced by chemical substitution in $Bi_2Sr_2(Ca_z,Y_{1-z})Cu_2O_{8+y}$. The samples with low Ca concentration are insulators [$d\rho/dT<0$ and $\lim_{T\to 0}\rho(T)=\infty$] with resistivity values up to 10^3 Ω cm at 100 K. As the Ca content increases, the absolute value of ρ decreases while the insulating behavior persists. But at a Ca content higher than a critical value $z_c=0.43$, the resistivity changes qualitatively. The temperature coefficient $d\rho/dT$ becomes positive ($\rho\sim T$), indicating metallic conduction. The system has transformed from an insulator to a metal. Surprisingly, none of the samples shows a finite value of ρ at $T\to 0$. Instead, all samples that show metallic conduction at high temperatures show superconductivity with T_c up to 90 K. To our knowledge nobody has so far succeeded in obtaining samples which show a finite resistance at $T\to 0$ (see, for example, Refs. 1, 2, 7, 8, 10, 11, and 30). At $T=0$, the samples are either superconductors with zero resistance or insulators with infinite resistance. The absence of purely metallic samples is even more surprising if the high T_c values are taken into account. Even the sample with $z=0.5$ (see

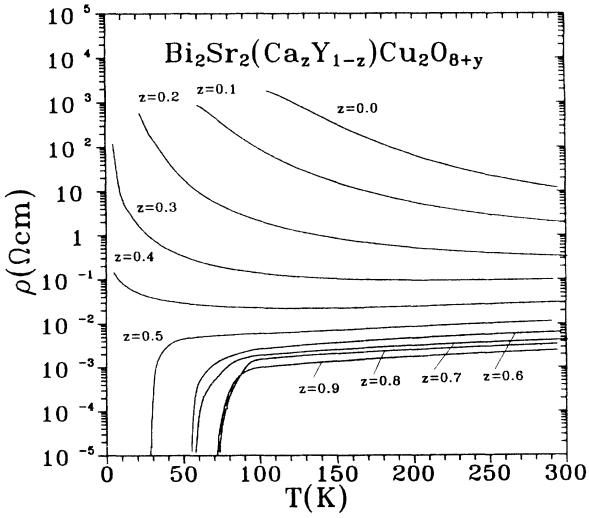

FIG. 1. Resistivity vs temperature for $Bi_2Sr_2(Ca_z,Y_{1-z})Cu_2O_{8+y}$ samples of different Ca content *z*. Note the transition from metallic and superconducting samples ($z\geq 0.5$) to insulating samples ($z\leq 0.4$) and the absence of samples with finite resistivity at $T\to 0$.

Fig. 1), which is very close to the IMT, still has $T_{c,\,\mathrm{mid}}=37$ K. This is a value higher than in any conventional superconductor.[3] The existence of an insulating and a superconducting region without an intermediate purely metallic region shows that the HTSC's are very unusual materials already in their normal state. As shown in Fig. 2, the superconducting transition temperature (T_c) rises with the Ca content in samples with $z>z_c$, reaching a maximum of $T_{c,\,\max}=90$ K at $z=(0.8\pm0.05)$ and then falls to $T_c=72$ K at $z=1.0$. This maximum is in agreement with the results of other groups.[5,7,8,10,12,30]

In order to understand the charge transport in this system and the influence of chemical doping, we have measured the Hall effect. Above T_c, the Hall coefficient R_H is almost constant with a weak temperature dependence which can be described by $R_H\simeq a+b/T$.[1,2] The temperature dependence of the Hall coefficient and its relation to the separation of spin and charge excitations in HTSC's proposed by Anderson[31] will be discussed separately.[17] The Hall coefficient is positive, indicating holelike charge carriers. In a one-band model, the carrier density p can be obtained from the Hall coefficient using $R_H=1/pe$. In Fig. 2 we show the dependence of the carrier density $p(z)$ calculated using the value of R_H at $T=200$ K, upon Ca content for metallic ($z>z_c$) samples of the system $Bi_2Sr_2(Ca_z,Y_{1-z})Cu_2O_{8+y}$. The hole density $p(z)$ increases with Ca content, in agreement with published results.[5,8,12] Taking the error bars into account, the increase is approximately linear. In the following we will therefore assume that the hole density and Ca content are linearly related to each other, at least in the metallic regime.

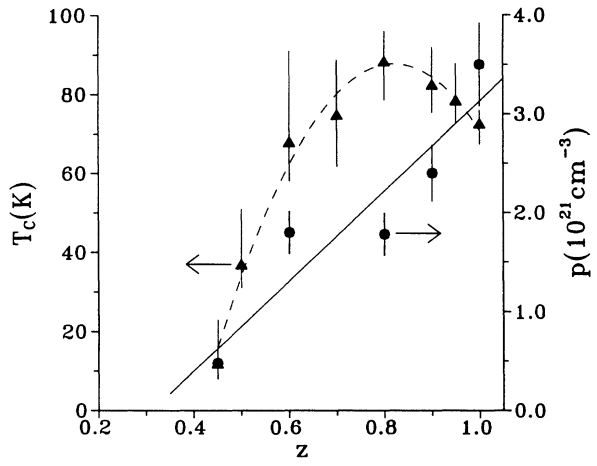

FIG. 2. Carrier density p (circles, left scale) and superconducting transition temperature T_c (triangles, right scale) vs Ca concentration z in $Bi_2Sr_2(Ca_z,Y_{1-z})Cu_2O_{8+y}$. The carrier density was derived from the Hall coefficient R_H at $T=200$ K using $p=1/R_He$. The solid line shows the expected linear relation $p\sim z$. The error bars mark the onset ($\rho=0.9\rho_n$) and offset ($\rho=0.1\rho_n$) of the superconducting transition. The dashed line is a guide to the eye.

IV. CHARGE TRANSPORT ON THE INSULATING SIDE OF THE IMT

The understanding of the charge transport in insulating samples is very important because it provides information about electronic correlations and the density of states. As it is seen in Fig. 1, the resistivity of insulating samples increases strongly with decreasing temperature below about 100 K. This increase cannot be described by thermally activated conduction, which would require a temperature dependence such as $\rho(T)\sim\exp[1/T]$. Instead, it can be described by hopping conduction[23] between localized states. In hopping conduction the temperature dependence is generally weaker than $\exp[1/T]$ and has been calculated for a number of different cases.[32] The best-known examples for hopping conduction are due to Mott and Davis[23] and Shklovskii and Efros.[22] For these two cases, the temperature dependence is

$$\rho(T)=\rho_0\exp\left\{\frac{T_0}{T}\right\}^{\alpha}, \tag{1}$$

where T_0 is a characteristic temperature which will be discussed later [see Eqs. (4) and (5)] and

$$\alpha=\frac{n+1}{n+D+1}. \tag{2}$$

D is the dimensionality of the hopping process, and n describes the energy dependence of the density of states $g(E)$ in the vicinity of the Fermi energy, which behaves like

$$g(E)\sim|E-E_F|^n. \tag{3}$$

For an energy-independent density of states ($n=0$), this leads to a Mott-Davis variable-range hopping case of $\alpha=\frac{1}{3}$ in two dimensions and $\alpha=\frac{1}{4}$ in three dimensions. Shklovskii and Efros have analyzed the case of low carrier concentration where electrons interact via the unscreened Coulomb potential, which leads to a gap in $g(E)$ that is pinned at E_F. They showed that in two dimensions $n=1$, whereas in three dimensions $n=2$. This leads to the same exponent $\alpha=\frac{1}{2}$ for two and three dimensions in (2).

The electrical resistivity of the $Bi_2Sr_2(Ca_z,Y_{1-z})Cu_2O_2$ system cannot be described by the simple Mott-Davis or Shklovskii-Efros case alone. The reason for this failure is probably that $g(E)$ has more structure within several times k_BT than is allowed for by (3) and changes significantly upon Ca substitution. The detailed behavior of $g(E)$ will be discussed later. Most reports in the literature have analyzed their data using only the abovementioned values of $\alpha=\frac{1}{4}$, $\frac{1}{3}$, and $\frac{1}{2}$, trying to extract the dimensionality of the conduction process from this fit.[10–12,16] We will use a more generalized approach where α is allowed to vary, and we will not address the question of dimensionality because the theoretical assumptions used in deriving the exponent $\alpha=\frac{1}{3}$ and $\frac{1}{4}$ in the Mott-Davis case of (2) are not fulfilled in HTSC's. The resistivity of six insulating samples of the Bi 2:2:1:2 system is shown in Fig. 3. The data are the same as in

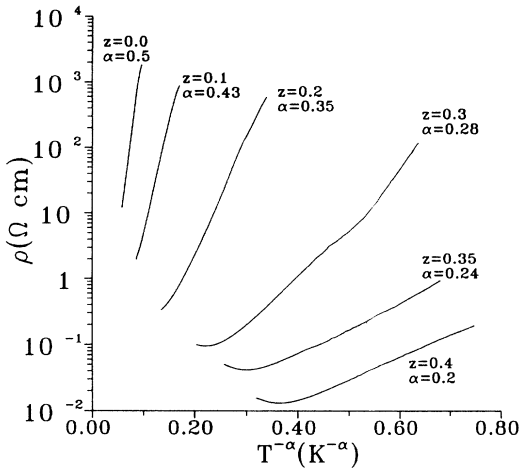

FIG. 3. Temperature dependence of the resistivity for samples in the insulating regime of $Bi_2Sr_2(Ca_z,Y_{1-z})Cu_2O_{8+y}$. The data are plotted on a logarithmic scale vs $T^{-\alpha(z)}$ to show the hopping character of the conduction (1). The $\alpha(z)$ values are different for all samples and are indicated next to the curves together with the respective Ca concentrations. The determination of the $\alpha(z)$ value is discussed in the text.

Fig. 1, but here they are plotted as $\ln(\rho)$ vs $T^{-\alpha(z)}$ to show the hopping behavior in agreement with (1).

The exponent α used for plotting the data in Fig. 3 is different for each of the six samples, causing the different starting point of the six curves on the $T^{-\alpha}$ axis. The determination of α for a given Ca concentration is rather difficult because of the strong exponential temperature dependence in (1), which almost masks the much weaker power-law dependence. Conventional fitting procedures are further complicated by deviations from the hopping conduction at high temperatures, which can be seen best for the $z=0.4$ sample. The physical reason for these deviations will be discussed later. They lead to both quite inaccurate values of α and unphysical variations of T_0 and ρ_0. We have therefore determined α differently.

For a given Ca concentration, the resistivity data were plotted as $\ln(\rho)$ vs $T^{-\alpha}$ with values of α between 0.15 to 0.6. The correct value of α is the one giving a straight line over the largest region in the low-temperature part. By this method, α can be determined with an estimated error of 10%. We have obtained values of $\alpha=(0.5\pm0.05)$ for $z=0$ and $\alpha=(0.2\pm0.02)$ for $z=0.4$ by this method. Because of the large error, we have not determined the α values for all Ca concentrations by this method. Instead, we have assumed $\alpha(z)$ to vary linearly between the two above-mentioned values. In view of the small absolute change in $\alpha(z)$, this seems a reasonable approximation. The fact that all six curves show reasonably straight lines in a resistance range of up to three orders of magnitude justifies our approach. The exponent $\alpha=(0.5\pm0.05)$ which we find for the sample $Bi_2Sr_2YCu_2O_{8+y}$ is in agreement with the Shklovskii-Efros case of a gap in $g(E)$. The same exponent has been observed by Mandrus *et al.*[11] in a Ca-deficient single crystal of $Bi_2Sr_2(Ca_{0.25},Y_{0.55})Cu_2O_{8+y}$. As the IMT is approached, the carrier density increases, which leads to better screening. Therefore the gap in $g(E)$ has to disappear and α has to become smaller than $\frac{1}{2}$. This is in agreement with the experimentally observed decrease to $\alpha=0.2$ at the IMT. The observed variation of $\alpha(z)$ explains the disagreement in the literature about the exponent in the hopping conduction for the $Bi_2Sr_2(Ca_z,R_{1-z})Cu_2O_{8+y}$ system and with it the disagreement about dimensionality.[10–12,16] Depending on the carrier concentration in the sample, very different values of α and therefore for the dimensionality can be obtained if only the Mott-Davis and Shklovskii-Efros cases are considered.

Another feature, easily seen in Fig. 3, is the decreasing slope of the curves as the Ca content increases. The slope is given by T_0^{α} (1) and is related to the localization radius a_H, which is the decay length of the localized carrier wave function. The exact relation between a_H and T_0 is known for the simple Mott-Davis ($D=3$) and the Shklovskii-Efros cases, respectively, where it is given by[23]

$$T_0 \simeq \frac{2.1}{k_B g(E_F) a_H^3} \tag{4}$$

and by[22]

$$T_0 \simeq \frac{2.8e^2}{4\pi\epsilon_0 k_B} \frac{1}{\epsilon a_H} . \tag{5}$$

Here ϵ is the static dielectric constant. In order to extract the localization radius from the experimental α and T_0 values for all Ca concentrations independent of D and n, we follow an approach developed by Moshchalkov and Muttik for doped semiconductors.[33]

The process of hopping conduction may be modeled by the behavior of a network of resistors[22] with the characteristic resistivity being determined by the resistivity of the critical percolating path:

$$\rho \sim \exp[\xi_c] . \tag{6}$$

The dimensionless variable ξ takes into account two possible conductivity channels arising from both wave-function overlap and thermal excitations:

$$\xi \equiv \frac{r_{ij}}{a_H} + \frac{E_{ij}}{k_B T} . \tag{7}$$

Here r_{ij} and E_{ij} are the distance and energy difference between sites i and j participating in the hopping process. The critical percolating path ξ_c is found from the percolation condition

$$VN = B_c^{(D)} , \tag{8}$$

where $B_c^{(D)}$ is a constant depending only on dimensionality D, V is the characteristic volume $V \sim r_{ij}^D$, and $N \sim (E_{ij})^{n+1}$ is the number of sites taking place in the conduction process, which is found from integrating the density of states (3). At $\xi=\xi_c$,

$$(r_{ij})_c^D (E_{ij})_c^{n+1} \sim B_c^{(D)} . \tag{9}$$

Inserting $(r_{ij})_c \sim (\xi_c a_H)$ and $(E_{ij})_c \sim \xi_c k_B T$ above, we obtain

$$(\xi_c a_H)^D (\xi_c k_B T)^{n+1} \sim B_c^{(D)} \tag{10}$$

and, with (1) and (6),

$$\rho \sim \exp\{\xi_c\} \sim \exp\left\{\left[\frac{T_0}{T}\right]^{\alpha}\right\}, \tag{11}$$

with

$$T_0 = \frac{\text{const}}{a_H^{[D/(n+1)]}}, \quad \alpha = \frac{n+1}{D+n+1} = \frac{1}{[D/(n+1)]+1}, \tag{12}$$

or

$$T_0 = \text{const}\, a_H^{[-D/(n+1)]}. \tag{13}$$

Taking the relation $D/(n+1) = (1-\alpha)/\alpha$ for the hopping exponent from (2), we get the relation

$$a_H \sim T_0^{[\alpha/(\alpha-1)]}. \tag{14}$$

This makes it possible to estimate the variation of the localization radius a_H with chemical composition using experimental T_0 and α values. The three particular cases ($n=0$, $D=3$; $n=1$, $D=2$; and $n=2$, $D=3$) discussed in (4) and (5) are also described by this expression. This simple method completely ignores a possible effect of the prefactor in (6) on the localization radius in (14). In addition, the coefficient of proportionality in (14) may also depend weakly upon the details of the density of states in the vicinity of E_F, besides the $B_c^{(D)}$ variation with dimensionality, which is known from percolation theory.[34] In spite of these shortcomings, (14) gives a good possibility to study the behavior of the localization radius a_H from resistivity measurements.

The variation of the localization radius a_H with Ca content is shown later (in Fig. 10 and discussed there). It diverges at the IMT, indicating that here the charge carriers get delocalized through increasing overlap between the wave functions on neighboring sites. In the following section, we will show that the characteristic quantities of the hopping transport, namely, α and T_0 in the insulating samples, are determined only by carrier density, which in our case is given by the Ca content.[15] To do so, we have investigated various samples where Y was replaced by other R elements. Their resistivity is shown in Fig. 4 as $\ln(\rho)$ vs $T^{-0.2}$ to show the hopping conduction.

The samples have the same nominal carrier concentration because they have the same content of trivalent Y or R ions. All samples give straight lines in the low-temperature region, showing that the transport is due to hopping and that the exponent is $\alpha = (0.2 \pm 0.02)$, independent of the R ions. This shows that the character of the hopping is the same for the three samples and is independent of the specific R ion separating the CuO_2 planes. In particular, it is independent of the magnetic moment of the R ion ($\mu_Y = 0$, $\mu_{Nd} = 3.5\mu_B$, $\mu_{Gd} = 8.5\mu_B$) and of the CuO_2-plane spacing, which is changed

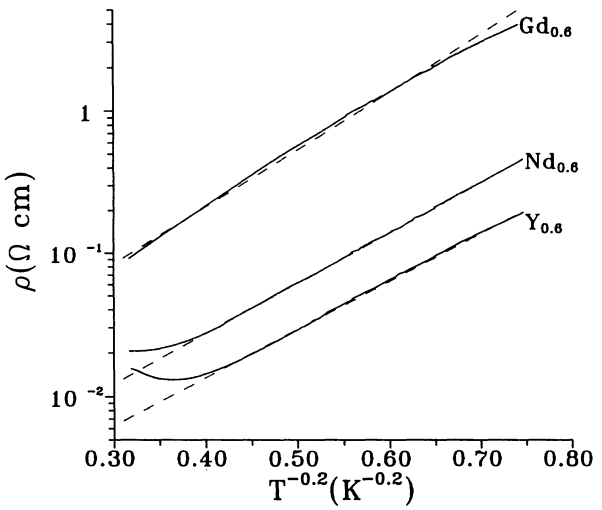

FIG. 4. Logarithmic plot of resistivity vs $T^{-0.2}$ showing the similarity in hopping conduction for $Bi_2Sr_2(Ca_{0.6},R_{0.4})Cu_2O_{8+y}$ with different R=(Gd, Nd, Y). Dashed lines are fits to (1) in the low-temperature regime.

significantly by substituting ions that differ by as much as 10% in their ionic radii ($r_Y = 0.893$ Å, $r_{Gd} = 0.938$ Å, $r_{Ca} = 0.990$ Å, $r_{Nd} = 0.995$ Å). The slope of all curves in Fig. 4 is the same within experimental error. The insensitivity of the slope T_0^{α} to the substituted RE ion shows that the localization radius which is given by (14) depends only upon the carrier density. The only quantity depending on the RE ion is the prefactor ρ_0 in (1), which increases by an order of magnitude when going from nonmagnetic Y to magnetic Gd. This dependence on the magnetic moment will be discussed elsewhere.[17]

V. DENSITY OF STATES

To study the electronic density of states and its dependence on the Ca content, we have performed ultraviolet photoemission spectroscopy (UPS) on both metallic and insulating samples. The UPS experiments were performed at room temperature. When attempting to extract the electronic density of states from UPS experiments, one has to keep in mind that in strongly correlated systems, such as HTSC's, the electronic density of states in the vicinity of E_F may be strongly temperature dependent. Nevertheless, for HTSC's, the relevant temperature scale should be given by the exchange interaction constant $J \simeq 1600\,\text{K} \gg 300\,\text{K}$. Therefore we can use the UPS spectra at 300 K as an estimate for the density of states at $T=0$.

The spectra of four samples with different compositions are shown in Fig. 5. Figure 5(a) shows the spectra down to a binding energy of 9 eV below E_F. The density of states at E_F is small for all samples. At higher binding energy, it rises and has a peak at approximately 3 eV. Studies of the resonance behavior of this peak show that these are dominantly Cu $3d$ states.[35,36] The shape of the peak is almost the same for all four samples, showing that these low-lying states are unaffected by Ca substitution.

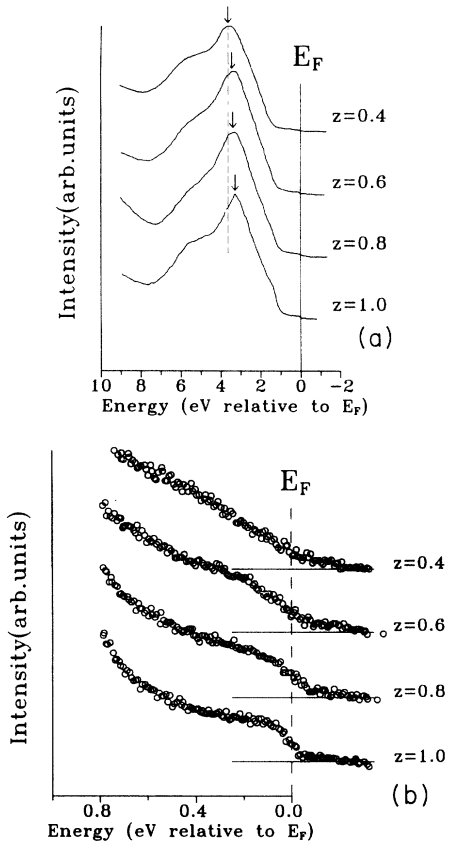

FIG. 5. UPS spectra for $Bi_2Sr_2(Ca_zY_{1-z})Cu_2O_{8+y}$ samples. (a) The arrows indicate the position of the peak at ~3 eV binding energy. The dashed line shows the position of the peak in the insulating sample with $z=0.4$. (b) Expanded view of the spectra in Fig. 6(a) near the Fermi level.

On the other hand, the distance of this peak relative to E_F, which is the zero energy for all spectra, clearly changes. The peak is closest to E_F for the metallic sample with $z=1$ and farthest away for the insulating sample $z=0.4$. Because these are relatively low-lying states and are due to Cu 3*d* orbitals, they should not shift their energetical position upon substitution at the Ca site. In UPS experiments the binding energy is measured relative to E_F. This means that the apparent shift of the 3-eV peak is in reality caused by a shift in the Fermi energy due to the change in carrier concentration. The insulating samples have a relatively low hole concentration, resulting in a Fermi energy sitting in the upper part of the highest occupied band. As the hole density is increased by substituting Ca^{2+} for Y^{3+}, the Fermi energy gets shifted deeper into the band and closer to the low-lying Cu 3*d* states at 3 eV binding energy. The shift is approximately 0.2 eV between the spectra of the $z=0.4$ and 1.0 samples and about 0.5 eV between $z=0$ and 1. This shift was not seen clearly in earlier photoemission experiments,[37,38] but has been observed to be qualitatively similar in a core and valence-band photoemission study by Golden *et al.*[39]

Because the same shift was also observed in a second set of samples [40] and the sample resistance is low ($R<10$ m Ω), we can exclude the possibility of electronic charging as a source of the shift.

The shift in E_F means that a rigid-band picture is a reasonable approximation at higher binding energies ($E>2$ eV).[40] On the other hand, we will now show that it is not a good approximation in the vicinity of the Fermi energy. This can be seen in Fig. 5(b), where we show a closeup view of the spectra in the vicinity of E_F. For the insulating sample ($z=0.4$), the spectrum shows a monotonically decreasing density of states with no structure near E_F. In contrast to this behavior, the metallic samples with higher hole concentration all show a hump at a binding energy of $\simeq 0.2$ eV on top of a decreasing background. This hump increases with Ca content and is best seen for $z=1$. It can be interpreted mainly as a narrow band of total width $\tilde{W}\simeq 0.6$ eV (occupied and unoccupied part),[40] which is formed upon hole doping. The intensity of this band increases with Ca content. It has also been observed by other authors,[37,38] and the width of the occupied part is agreed upon to be approximately 0.3 eV. This narrow band is present in all *p*-type HTSC's investigated with UPS or electron-energy-loss spectroscopy (EELS).[9,41] More indirect evidence for the existence is also found in the optical conductivity[13,42] and Raman scattering.[43] EELS experiments have shown that this narrow band has predominantly O 2*p* character[9,35,36] and lies mostly in the CuO_2 plane.[9,38,44] Because this narrow band is situated at the Fermi energy, it will contribute to the dc conductivity, and as it is observed in all HTSC compounds, it is most probably linked to their superconductivity. In the UPS spectra, the intensity of the narrow band rapidly decreases in the insulating samples, but the band probably persists down to very low Ca concentrations. Here it will be difficult to observe because of its low intensity and a narrowing caused by the decreasing interaction among the states in the band.

The fact that the intensity of this band increases with the hole concentration has important consequences for the nature of the band which has been under intense theoretical investigation.[45–49] The question is whether the band is formed by conventional impurity states like in doped semiconductors or by highly correlated electron states inherent to the CuO_2 plane. In doped Si, for example,[22,24] where the carrier concentration is at most $\sim 10^{18}$ cm^{-3}, impurities with initially sharp energy levels form a band as a result of their mutual interaction, which causes a statistical energy spread. This band is extremely narrow ($W\sim 0.1$ meV).[22] The bandwidth of $\tilde{W}\simeq 0.6$ eV observed in the HTSC's is orders of magnitude larger. There are two possible reasons for the increased bandwidth. First, the interaction among the carriers will be higher because the carrier density is orders of magnitude higher. Second, the disorder is higher in HTSC's because a large fraction of the Y atoms are exchanged. This disorder will also broaden the band.[22] In this impurity model, the growth of intensity for the narrow band at E_F is a very natural feature.

A different approach, heavily investigated by theorists, deals with a singlet which is formed by the interaction of a hole doped on the O 2*p* orbital which interacts with the hole in the *d* orbital of the Cu^{2+} ion. The singlet state

consists of the Cu^{2+} spin in the center of a square of oxygen ions and is compensated by an oxygen hole spin shared among the four corners.[47] This so-called Zhang-Rice singlet also results in a narrow-band-like state at the Fermi level for the doped system.[46] The question of how the intensity of this singlet state grows as the system is doped with holes has to our knowledge not been investigated in detail so far. Such an investigation would be very helpful for an understanding of the nature of the states at E_F in HTSC's.

Before discussing our narrow-band model, we would like to come back to the temperature dependence of the resistivity for samples with $z \lesssim z_c$. As can be seen in Fig. 6, these samples are insulators [$d\rho/dT<0$, $\rho(T\rightarrow 0)=\infty$] at low temperatures where they show hopping conduction as was shown in Fig. 3. Above a crossover temperature $T_{\min}$, which is indicated by arrows, the resistivity becomes metallic ($\rho \sim T$). The slope of the metallic resistivity $d\rho/dT$ decreases with increasing Ca content from $d\rho/dT=7.98\times10^{-5}$ at $z=0.3$ to $d\rho/dT=6.75\times10^{-6}$ at $z=1$. The sample with $z=1$ is not shown in Fig. 6. It changes continuously through the IMT, which shows that the process leading to the $\rho \sim T$ behavior is the same in the superconducting and insulating samples. The crossover in the resistivity has also been observed by other groups for this system[11,12,30] and also in $(La,Sr)_2CuO_4$,[20] but its origin has not been discussed so far.

The crossover from hopping to metallic conduction for samples slightly below the IMT ($z \lesssim z_c$) is easily explained if the disorder in this system is taken into account. Disorder is presented in this system because of the random occupation of the sites between the CuO_2 planes by Ca or Y. As shown by Anderson,[50] the presence of weak disorder in a periodic system causes the localization of the electronic states in the tails of the conduction band. Therefore, in one and the same band, localized states which conduct by hopping will coexist with delocalized states that show metallic conduction. The energy separating the delocalized from the localized states is called the mobility edge E_c. The factor determining the character of conduction is then the position of E_F with respect to E_c.

We now propose a schematic picture for the develop-

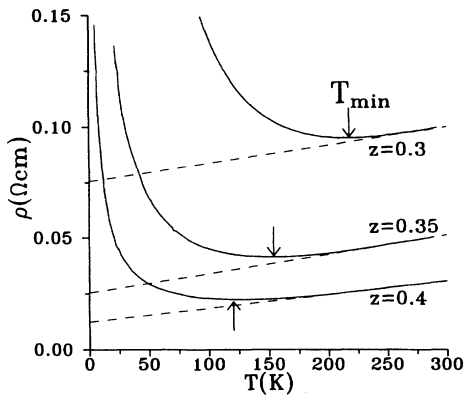

FIG. 6. Resistivity vs temperature for $Bi_2Sr_2(Ca_z,Y_{1-z})Cu_2O_{8+y}$ samples with z below the critical concentration for the IMT ($z_c=0.43$). The dashed lines are fits to the metallic resistivity $\rho \sim T$ at high temperature. The crossover from metallic to hopping conduction $\rho \sim \exp[T^{-\alpha}]$ at $T_{\min}$ is indicated by arrows.

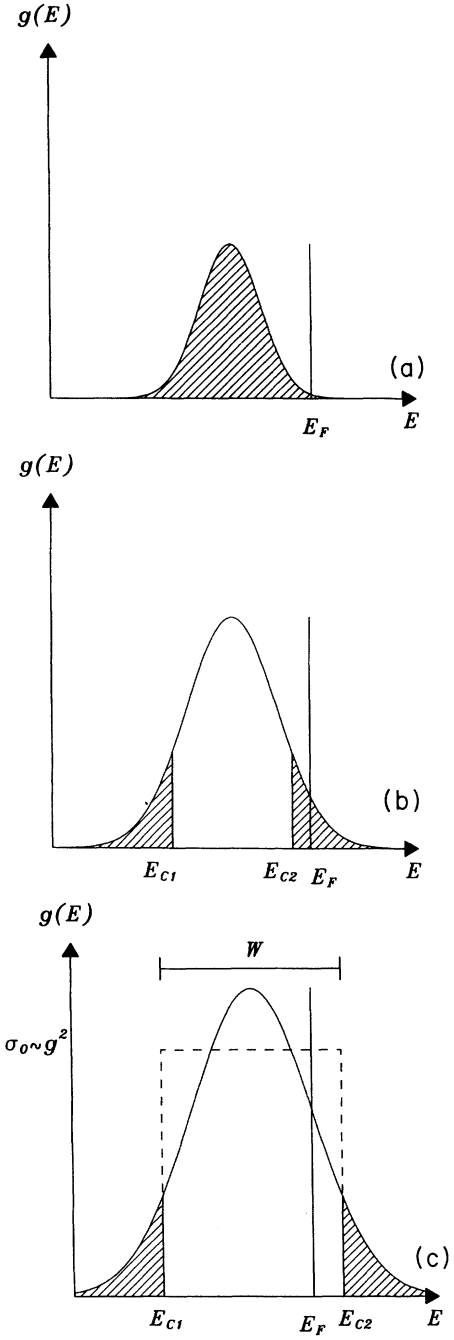

FIG. 7. Schematic electronic density of states $g(E)$ of the conduction band for high-temperature superconductors at three different levels of hole doping. The vertical scale is the same for all three curves. Localized states are shaded. (a) Low hole doping, insulating samples. All states are localized. (b) Intermediate doping just below the critical concentration for the insulator-metal transition. (c) High doping, metallic, and superconducting samples. The dashed line indicates the rectangular band assumed in our model calculation.

ment of the density of states around E_F as one moves from the insulating to the metallic regime by chemical substitution. All states at higher or lower binding energy are omitted for simplicity. The schematic picture is based on the data of the Hall effect, electrical resistivity, UPS, and the above-mentioned disorder. Figure 7 shows the density of states for three levels of doping. Our schematic picture is an extension of the picture proposed by Matsuyama *et al.*[38] and includes effects of disorder[51] and the experimentally observed shift of the Fermi energy.

As was seen in the UPS spectra, the maximum of the narrow band lies below E_F, which is also in agreement with the holelike conduction observed in the Hall effect. The band will have a domelike shape, and there will be a region of localized states below E_{c_1} and above E_{c_2} due to disorder. The case of a sample deep in the insulating regime with very low carrier concentration is shown in Fig. 7(a). Here all states are localized. Since the localization radius a_H is small compared to the carrier separation ($d_{(e^+,e^+)} \simeq p^{1/D}$), the interaction among the carriers is weak and the band is narrow.[22] There are no delocalized states in this case, and conduction can only take place by hopping between localized states within $k_B T$ around E_F, in agreement with the results of Fig. 3. The existence of a Coulomb gap has been neglected in Fig. 7(a) for simplicity.

The situation at higher doping, slightly below the IMT, is shown in Fig. 7(b). The smaller carrier separation leads to a larger overlap integral between the carrier states, and therefore a narrow region of delocalized states appears in the band center. The increased interaction among the carriers and the larger disorder both lead to an increase of the bandwidth. The Fermi energy has moved closer to the band center as evidenced by UPS and thus gives a higher carrier density in the Hall effect. Because E_F is still in the localized part of the band, we observe hopping conduction at low temperatures. At higher temperatures, where, because of a broadening of the Fermi distribution, delocalized states become accessible, the situation changes. The delocalized states have a much higher mobility and will therefore dominate the conduction, leading to a metallic resistivity ($\rho \sim T$) at sufficiently high temperature ($k_B T \geq E_F - E_{c_2}$). This explains the crossover of the resistivity shown in Fig. 6.

The difference $E_F - E_c$ can be calculated from the data by two methods. For samples showing a resistance minimum, we have used the relation

$$k_B T_{\min} = E_F - E_c \ . \tag{15}$$

For samples not showing the resistance minimum, we have made use of the fact that the resistivity just below the crossover at $T_{\min}$ will show thermally activated behavior across the mobility gap which is equal to $(E_F - E_c)$. The only assumption made here is that the mobility of the localized states is very small compared to that of the delocalized states. We can then determine $E_c - E_F$ by fitting the resistivity to

$$\rho(T) = \rho_0 \exp\left\{ \frac{(E_F - E_c)}{k_B T} \right\} . \tag{16}$$

This procedure was adopted for $z < 0.3$ in the temperature range $400 < T < 600$ K and gives values that match well the values obtained by using (15). (The results will be discussed in conjunction with Fig 10.) The resistance minimum and thermally activated behavior of $\rho(T)$ in a certain temperature region in this system were also observed by Mandal *et al.*[12] They did not link the two facts and explained the thermally activated behavior by polaronic conduction. Their values for the polaronic activation energy gap agree with our values of $(E_c - E_F)$ within 10%. We think our explanation based on the existence of a mobility edge is more natural because it links the observed resistance minimum, the thermally activated behavior, and the hopping conduction assuming only disorder, which in a chemically substituted system such as HTSC's is out of the question. It also explains the absence of a resistance minimum for samples with $z < 0.2$, because here the minimum is shifted to very high temperatures. The good agreement between our data and those of Mandal *et al.* shows that the position of the mobility edge E_c is determined by intrinsic disorder and only weakly influenced by sample preparation and quality.

The third schematic density-of-states picture in Fig. 7(c) shows the band for a metallic sample. These are the samples that show superconductivity. The intensity of the band has increased, as suggested by the UPS results. The width has further broadened because of even stronger interaction among the doped carriers and the larger disorder. The increased hole concentration has moved E_F into the delocalized part of the band. The system is therefore a metallic conductor. If the system was even further doped, the Fermi energy would eventually move below the band center, resulting in electronlike conduction as observed in heavily doped (La,Sr) CuO_4.[1,21]

VI. NARROW-BAND MODEL

In the following we present a simple model which qualitatively reproduces the observed IMT, the crossover from insulating to metallic resistivity, and the linear resistivity for the metallic samples. The model was first proposed by Moshchalkov[51] and enables the calculation of the temperature-dependent conductivity $\sigma(T)$ from a very simple model function for the energy-dependent conductivity $\sigma(E)_{T=0}$, which is proportional to the square of the electronic density of states.

The calculation is done using the Kubo-Greenwood formula, which is valid for both $l \sim d_{(e^+,e^+)}$, and $l \gg d_{(e^+,e^+)}$ where l is the mean free path[23] and $d_{(e^+,e^+)}$ the carrier-carrier separation. It therefore covers the entire IMT from samples showing hopping conduction where $l \sim d_{(e^+,e^+)}$ to metallic samples with weak scattering $l \gg d_{(e^+,e^+)}$. We are interested in the transport properties up to a few hundred degrees kelvin; therefore, we need to consider only the states in the vicinity of E_F. All states at higher energy are neglected. We assume that

the density of states can be modeled by a rectangular band of width $W=(E_{c1}-E_{c2})$ and constant height $\sigma_0 \sim \langle g(E)^2 \rangle$, as is shown by the dashed lines in Fig. 7(c). The width of this mobile band W is obviously smaller than the bandwidth $\tilde{W}$ observed in the UPS experiments. The assumption of a rectangular band neglects the mobility of the localized states in the band tail. A finite mobility could be included, but would only increase the number of free parameters without giving qualitatively new information. For simplicity, the height of the band σ_0 is taken to be independent of the Ca content z. This is in disagreement with the UPS results, which showed an increase of the narrow band with Ca content, but as this increase cannot be determined precisely from the experiments, we have ignored it. Thus we use an energy-dependent conductivity of the form

$$\sigma(E)=\begin{cases}\sigma_0, & -W \le E \le 0 \\ 0, & \text{elsewhere}\end{cases} . \tag{17}$$

The zero energy is taken at the upper band edge, leading to $W<0$. Therefore $E_F>0$ means a Fermi energy outside of the conduction band corresponding to Figs. 7(a) and 7(b) and $E_F<0$ means a Fermi energy within the conduction band corresponding to Fig. 7(c). In this model a temperature-dependent Fermi level $E_F(T)$ need not be taken into account because, if the narrow band arises from electron-electron correlations, it is pinned at E_F and all shifts of E_F with temperature are followed by a corresponding shift of the narrow band. The temperature dependence $\sigma(T)$ is related to the energy dependence $\sigma(E)$ by the Kubo-Greenwood formula[23]

$$\sigma(T)=-\int_{-\infty}^{+\infty}\sigma(E)\frac{df(E,E_F)}{dE}dE . \tag{18}$$

Here $f(E,E_F)$ is the Fermi distribution function. Inserting $\sigma(E)$ from (17), the integral transforms into a sum:

$$\sigma(T)=\sigma_0\left\{\frac{1}{\exp\left\{-E_F/k_BT\right\}+1}-\frac{1}{\exp\left\{(W-E_F)/k_BT\right\}+1}\right\} . \tag{19}$$

Equation (19) contains the entire information about the temperature and composition dependence of the resistivity in our model.

We have to distinguish the cases where E_F is larger or smaller than zero. Both can be treated in a high- and a low-temperature approximation. Numerical results of (19) are shown in Fig. 8 for a bandwidth $W=1$ and E_F as a parameter.

We first discuss the metallic case ($E_F<0$). Using a high-temperature approximation [$E_F \ll k_BT$ and $(W-E_F) \ll k_BT$], we get

$$\rho(T)=\frac{1}{\sigma(T)} \simeq \frac{4k_B}{\sigma_0(-W)}T . \tag{20}$$

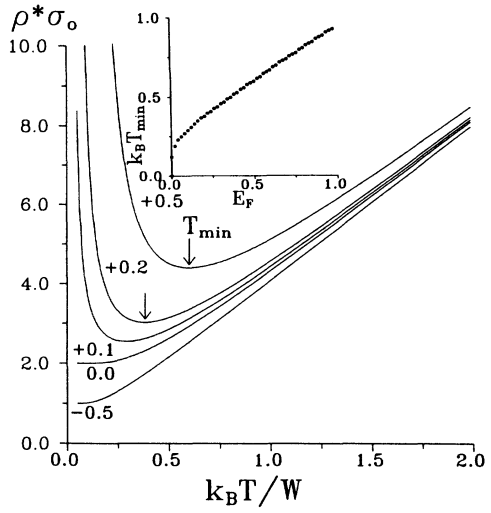

FIG. 8. Resistivity ρ multiplied by σ_0 vs temperature calculated for a narrow rectangular band of width $W=1$ using (19). The distance of the Fermi level relative to the upper band edge is indicated next to the curves and corresponds to Fig. 7(c). The arrows indicate the resistance minimum at $T_{\min}$. The inset shows numerical results for the variation of $T_{\min}$ with the position of the Fermi level.

The resistivity should therefore increase linearly with temperature, a behavior that is not only observed in $Bi_2Sr_2(Ca_z,Y_{1-z})Cu_2O_{8+y}$, but also in all other HTSC's.[1,2,26] The slope of the linear resistivity depends on the product $(W\sigma_0)$. If the band is only determined by the properties of the doped CuO_2 plane, then the slope should be independent of the surrounding crystal structure and depend on the carrier density via σ_0. This is in good agreement with the fact that the value $d\rho/dT$ for the linear resistivity is very similar for all HTSC compounds.

Next, we discuss the insulating case $E_F>0$ when the Fermi level is above but not too far from the mobility edge. In the low-temperature approximation ($E_F \gg k_BT$), we get

$$\rho(T) \simeq \frac{1}{\sigma_0}\exp\left\{\frac{E_F}{k_BT}\right\} . \tag{21}$$

The resistivity should therefore rise exponentially at low temperatures. The experimentally observed hopping conductivity with an increase weaker than $1/T$ can also be obtained if the finite mobility of the localized states outside of the rectangular band is taken into account. In the high-temperature limit ($E_F \ll k_BT$) of Eq. (19), we again recover the linear dependence of (20). The crossover from exponential to linear temperature dependence in the numerical results is indicated by an arrow in Fig. 8. It can be compared to the observed behavior which was shown in Fig. 6. The inset of Fig. 8 shows numerical results for the variation of $T_{\min}$ with E_F at $W=1$. It is seen that $T_{\min}$ is proportional to E_F for not too small

values of E_F, justifying our assumption in (15).

The numerical results in Fig. 8 can be compared to the experimental results in Figs. 1 and 6. Keeping in mind the simplicity of the model, the agreement is surprisingly good. The linear resistivity at high temperatures, the upturn toward $T=0$, and the minimum, which shifts toward higher temperature as the samples become more insulating, are all well reproduced. Superconductivity is obviously not contained in the model as there exists no attractive potential. Although the qualitative agreement is good, the quantitative agreement is not so good. The numerical results show a linearly increasing resistivity for $T>\frac{1}{2}W$, as seen in Fig. 8. If we use the estimated bandwidth from UPS experiments, which is about $\tilde{W}=0.5$ eV, and take into account that only the mobile states in the band center contribute to the linear resistivity, we can estimate a bandwidth of $W\simeq 0.2$ eV $\leq \tilde{W}$. This would mean that the linear resistivity should only be found above $T\simeq 1000$ K. This value is an order of magnitude higher than the experimentally observed lower limit for the linear temperature dependence of about 100 K. Whether this discrepancy indicates that only a very small fraction of the band observed with UPS is mobile ($W\sim 0.01$ eV $\ll \tilde{W}$), as has been suggested,[52] or whether this is a failure of the model remains to be seen.

VII. SCALING DEPENDENCE OF THE CONDUCTIVITY

From the IMT in doped semiconductors,[22] it is well known that the conductivity in the vicinity of the IMT obeys a scaling law

$$\sigma(z)=\sigma_0\left\{\frac{z-z_c}{z_c}\right\}^{\eta}, \tag{22}$$

with a critical exponent η, which can be calculated using the scaling theory which was first proposed by Abrahams *et al.*[53] The parameter z in (22) is normally taken to be the carrier concentration in the system. In the following analysis, we will assume that in $Bi_2Sr_2(Ca_z,Y_{1-z})Cu_2O_{8+y}$ we can replace the carrier density by the Ca concentration z. This assumption is supported by the linear dependence of the Hall coefficient R_H on the Ca content z in the metallic regime, which was shown in Fig. 2. The exponent η is unique for the character of the transition and independent of the specific substance under investigation. Therefore the critical exponent provides important information about the mechanism inducing the IMT. The determination of the scaling behavior in HTSC's is somewhat more complicated than in traditional semiconductors because, first, the conductivity at $T=0$ is needed in (22) and, second, the sample quality is not yet comparable to that of traditional semiconductors. As the conductivity at $T=0$ is not accessible because of the occurrence of superconductivity in all metallic samples, we have used the conductivity at $T=100$ K, which is the lowest temperature where the results are not influenced by the superconductivity, to search for scaling behavior. The results are shown in Fig. 9 in a double-logarithmic plot as conductivity $\sigma(T=100$ K) vs reduced concentration $\{(z-z_c)/z_c\}$ ($z_c=0.43\pm 0.02$) to show the power-law behavior. The solid circles are our results, and the open circles are values taken from the work of Mandrus *et al.*[11] The error in z_c can be estimated from the fact that the sample with $z=0.45$ is metallic and shows superconductivity and the sample with $z=0.4$ is insulating at low temperature. Thus we get $z_c=(0.43\pm 0.02)$. For the data of Mandrus *et al.*, we have used a critical concentration $z_c=0.42$. This value gives the best agreement with a power law and is in very good agreement with our value. Both data sets show a power-law behavior, proving that the conductivity in the $Bi_2Sr_2(Ca_z,Y_{1-z})Cu_2O_{8+y}$ system obeys a scaling law. The critical exponent is approximately $\eta=1$ for both data sets. Although the data sets agree remarkably well in their functional dependence and their critical exponent, there is a disagreement in the absolute conductivity. The data by Mandrus *et al.* have a conductivity almost a factor of 10 higher than our data and than other data published in the literature.[12,30] This could be due to the fact that they have used single-crystalline samples, which eliminates scattering from grain boundaries and gives a higher absolute conductivity. The fact that their data also show a scaling law with the same critical exponent $\eta=1$ is evidence for the universality of the scaling behavior. The value $\eta=1$ is the same as is observed in amorphous metals such as Nb:Si,[25] which have a rather wide conduction band and where the IMT is believed to be disorder induced. In contrast, narrow-band systems such as Si:P,[24] where the IMT is thought to be induced by Coulomb correlations, show $\eta=\frac{1}{2}$. This underlines the importance of disorder for the IMT in HTSC's.

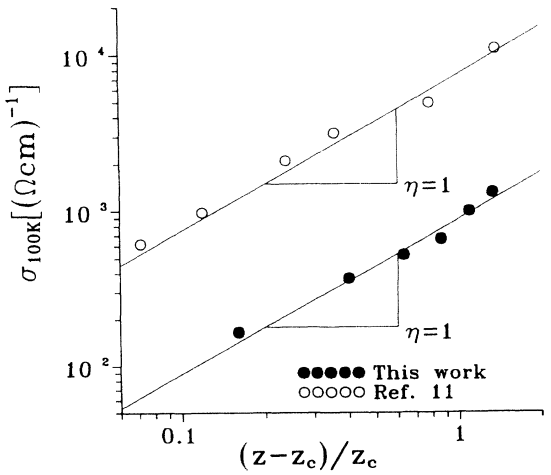

FIG. 9. Double-logarithmic plot of conductivity at $T=100$ K vs reduced Ca concentration for $Bi_2Sr_2(Ca_z,Y_{1-z})Cu_2O_{8+y}$. Solid circles are data from this work with $z_c=0.43$. Open circles are data taken from Mandrus *et al.* (Ref. 12) with $z_c=0.42$.

VIII. BEHAVIOR OF CHARACTERISTIC QUANTITIES AT THE INSULATOR-METAL TRANSITION

In Fig. 10 we present a summary of our results concerning the IMT in $Bi_2Sr_2(Ca_z,Y_{1-z})Cu_2O_{8+y}$. Shown are the mobility gap (E_c-E_F), the localization radius a_H, normalized to the value at $z=0$, and the conductivity in the metallic state at $T=100$ K ($\sigma_{100\,K}$). These three parameters are all plotted versus the Ca content z, which was shown to be proportional to the carrier concentration (see Fig. 2). The dashed lines are guides to the eye. The solid line shows the scaling law for the conductivity. Starting at $Bi_2Sr_2YCu_2O_{8+y}$ ($z=0$), the system is a charge-transfer insulator. By doping Ca^{2+} for Y^{3+}, we introduce hole states into the charge-transfer gap. For low z the localization radius of these doped states is very small, leading to negligible wave-function overlap and hopping conduction. As the hole density increases, E_F moves toward the band center. At the same time, the localization radius grows, leading to a larger overlap integral between the carriers and thereby moving E_c into the band tail. Thus the mobility gap (E_c-E_F) is reduced by doping. At the critical concentration $z_c=0.43$, the Fermi level reaches the mobility edge and the localization radius diverges. This leads to carrier states which extend over the entire crystal and to metallic conduction. These delocalized states become superconducting at low temperatures. The system has changed from a charge-transfer insulator to a high-temperature superconductor. The separation between the insulating region to the left and the metallic region to the right is marked by the vertical dashed line. As even more holes are introduced by further Ca doping, the absolute value of the metallic conductivity rises linearly. As shown in Fig. 2, the superconducting transition temperature T_c also rises, reaches a maximum of $T_c=90$ K at $z=0.2$, and then drops to $T_c=85$ K at $z=1.0$ despite the still rising conductivity. The disappearance of the mobility gap (E_c-E_F), the divergence of the localization radius a_H, and the vanishing metallic conductivity $\sigma_{100\,K}$ at z_c all are consistent with each other.

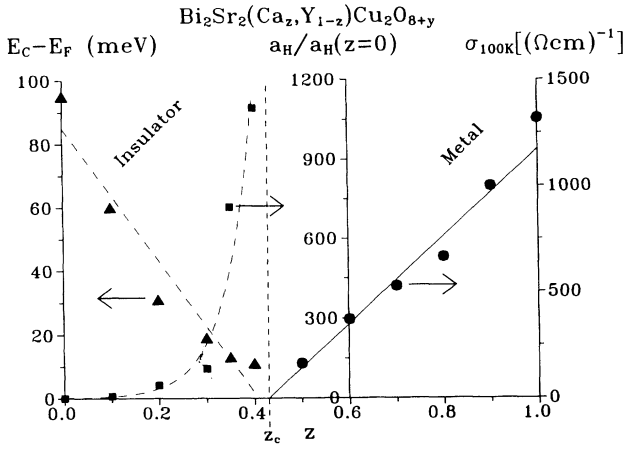

FIG. 10. Plot showing the disappearance of the mobility gap (E_c-E_F) (triangles), the divergence of the localization radius a_H (squares), and the linearly vanishing conductivity $\sigma_{100\,K}$ (circles) at the insulator-metal transition in $Bi_2Sr_2(Ca_z,Y_{1-z})Cu_2O_{8+y}$. The dashed vertical line separates insulating samples on the left from metallic samples on the right side. The values for the localization radius are normalized to the value at $z=0$. The solid line shows the scaling law for $\sigma(z)$ [Eq. (22)] with $\eta=1$, $z_c=0.43$, and $\sigma_0=890\,(\Omega\,\mathrm{cm})^{-1}$.

An important question remaining is whether this IMT is driven by Coulomb correlations and therefore of the Mott-Davis type[23] or by disorder and of the Anderson type.[22,50] As discussed above, the UPS spectra give clear evidence of a Fermi level which is shifted through a rather rigid-band structure by doping. In addition, the temperature dependence of the resistivity for samples close to the IMT, which is of the hopping type below and metallic above T_{min}, shows the coexistence of delocalized states in the band center with localized states in the band tail. These two results both point toward disorder-induced localization. Furthermore, the critical exponent $\eta=1$ is the same as in amorphous metals where the IMT is believed to be disorder induced. The insulator-metal transition in $Bi_2Sr_2(Ca_z,Y_{1-z})Cu_2O_{8+y}$ is therefore most likely caused by disorder and of the Anderson type, although the existence of a correlation gap can at the present not completely be excluded.

IX. CONCLUSION

Doping of Ca^{2+} in $Bi_2Sr_2(Ca_z,R_{1-z})Cu_2O_{8+y}$ induces holelike carriers and leads to an insulator-metal transition above a critical concentration $z_c=(0.43\pm0.02)$ (R=Y). All metallic samples show superconductivity with a maximum $T_c=90$ K at $z=(0.8\pm0.05)$. The insulating samples show hopping conduction $\rho\sim\exp[T^{-\alpha}]$ with an exponent α depending only on the carrier concentration and not on the specific R ion. Samples with a carrier concentration slightly below z_c show a crossover from hopping conduction at low temperatures to metallic conduction at high temperatures. This is evidence for the presence of localized states in the band tail due to disorder. Ultraviolet photoemission spectroscopy shows the appearance of new states at the Fermi level upon Ca^{2+} doping accompanied by a shift of the Fermi energy by 0.5 eV between $z=0$ and 1. A model is presented which describes the temperature-dependent conductivity, based on a density-of-states picture derived from the photoemission data. This model qualitatively explains the insulator-metal transition and the metallic resistivity in high-temperature superconductors. In the metallic regime of this insulator-metal transition, the conductivity obeys a scaling law with a critical exponent $\eta=1$. In the insulating regime, the localization radius diverges and the separation between localized states and the Fermi energy vanishes for $z\to z_c$. The insulator-metal transition is disorder induced and accompanied by a shift of the Fermi energy. It is therefore most probably of the Anderson type.

ACKNOWLEDGMENTS

This work was supported by Bundesministerium für Forschung und Technologie, Grants Nos. 13N5487A and 05 401 AAI, and by Arbeitsgemeinschaft Hochtemperatur-Supraleitung in Nordrhein-Westfalen. V.V.M. would like to acknowledge support from the Katholieke Universiteit Leuven and the Belgian High Temperature Superconductivity Impulse and Concerted Action Programs.

*Present address: Laboratorium voor Vaste Stof-Fysika, Katholieke Universiteit Leuven, Celesteijnenlaan 200D, B-3001 Heverlee, Belgium.

[1]N. P. Ong, in *Physical Properties of High-Temperature Superconductors II,* edited by D. M. Ginsberg (World Scientific, Singapore, 1990).

[2]Y. Iye, in *Physical Properties of High Temperature Superconductors,* edited by D. M. Ginsberg (World Scientific, Singapore, 1992), and references therein.

[3]J. C. Phillips, *Physics of High-T_c Superconductors* (Academic, San Diego, 1989).

[4]H. Maeda, Y. Tanaka, and M. Fukutomi, Jpn. J. Appl. Phys. **27**, L209 (1988).

[5]J. Clayhold, S. J. Hagen, N. P. Ong, J. M. Tarascon, and P. Barboux, Phys. Rev. B **39**, 7320 (1989).

[6]J. M. Tarascon, P. Barboux, G. W. Hull, R. Ramesh, L. H. Green, M. Giroud, M. S. Hedge, and W. R. McKinnon, Phys. Rev. B **39**, 4316 (1989).

[7]K. Koyoma, S. Kanno, and S. Nogouchi, Jpn. J. Appl. Phys. **28**, 1354 (1989).

[8]T. Han, A. Sawa, H. Uwe, and T. Sakudo, in *Proceedings of the 3rd International Symposium on Superconductivity,* Sendai, Japan, edited by K. Kajimura and H. Hayakawa (Springer, Tokyo, 1991).

[9]N. Nücker, H. Romberg, M. Alexander, and J. Fink, in *Studies of High Temperature Superconductors,* edited by A. Narlikar (Nova Sciences, City, 19xx), and references therein.

[10]T. Tamegai, A. Watanabe, K. Koga, and Y. Iye, Jpn. J. Appl. Phys. **28**, L1074 (1988); T. Tamegai, K. Koga, K. Suzuki, M. Ichihara, F. Saki, and Y. Iye, *ibid.* **28**, L112 (1989).

[11]D. Mandrus, L. Forro, C. Kendziora, and L. Mihaly, Phys. Rev. B **44**, 2418 (1991).

[12]P. Mandal, A. Poddar, B. Ghosh, and P. Choudhury, Phys. Rev. B **43**, 13 102 (1991).

[13]I. Terasaki, T. Nakahashi, S. Takebayashi, A. Maeda, and K. Uchinokura, Physica C **165**, 152 (1988).

[14]N. Fukushima, H. Niu, and K. Ando, Jpn. J. Appl. Phys. **27**, 1354 (1988).

[15]C. Quitmann, M. Fleuster, C. Jarchow, D. Andrich, P. L. Paulose, and G. Güntherodt, Physica C **185-189**, 1337 (1991).

[16]R. Yoshizaki, Y. Saito, Y. Abe, and H. Ikeda, Physica C **152**, 408 (1988).

[17]C. Quitmann, D. Andrich, B. Beschoten, and G. Güntherodt (unpublished).

[18]J. Zaanen, G. A. Sawatzky, and J. W. Allen, Phys. Rev. Lett. **55**, 431 (1985).

[19]J. B. Torrance, P. Lacorret, C. Asararoengehai, and R. M. Metzger, J. Solid State Chem. **93**, 567 (1991).

[20]H. Takagi, T. Ido, S. Ishibashi, M. Uota, S. Uchida, and Y. Tokura, Phys. Rev. B **40**, 2254 (1989).

[21]S. Uchida, H. Takagi, and Y. Tokura, Physica C **162-164**, 1677 (1989).

[22]B. I. Shklovskii and A. L. Efros, in *Electronic Properties of Doped Semiconductors,* edited by M. Cardona, P. Fulde, and H.-J. Queisser, Springer Series in Solid-State Sciences (Springer, Berlin, 1984), and references therein.

[23]N. F. Mott and E. A. Davis, *Electronic Processes in Non-Crystalline Materials,* 2nd ed. (Clarendon, Oxford, 1979), and references therein.

[24]M. A. Paalanen and R. N. Bhatt, Physica B **169**, 223 (1991).

[25]G. Hertel, D. J. Bishop, E. G. Spencer, J. M. Rowell, and R. C. Dynes, Phys. Rev. Lett. **50**, 743 (1983).

[26]M. Gurvitch and A. T. Fiory, Phys. Rev. Lett. **59**, 1337 (1987).

[27]G. A. Sawatzky, in *Earlier and Recent Aspects of Superconductivity,* edited by J. G. Bednorz and K. A. Müller, *Springer Series in Solid State Physics* (Springer, Berlin, 1990).

[28]K. Yvon and M. Francois, Z. Phys. B **76**, 413 (1989).

[29]S. A. Sunshine, L. F. Schneemeyer, D. W. Murphy, R. J. Cava, B. Batlogg, R. B. van Dover, R. M. Fleming, S. H. Glarum, R. Farrow, J. J. Krajewski, S. M. Zahurak, J. V. Waszczak, J. H. Marshall, P. Marsh, L. W. Rupp, Jr., and W. F. Peck, Phys. Rev. B **38**, 893 (1988).

[30]T. Onozuka, Y. Iwabuchi, T. Fukase, H. Sato, and T. E. Mitchell, Phys. Rev. B **43**, 13 066 (1991).

[31]P. W. Anderson, Phys. Rev. Lett. **67**, 2092 (1991).

[32]See, for example, *Proceedings of the Fourth International Conference on Hopping and Related Phenomena, Marburg, 1991* [Philos. Mag. **65**, (1992)].

[33]V. V. Moshchalkov and I. G. Muttik, Fiz. Tverd. Tela (Leningrad) **28**, 3750 (1986) [Sov. Phys. Solid State **28**, 2114 (1986)].

[34]J. W. Essam, in *Phase Transitions and Critical Phenomena,* edited by C. Domp and M. Green (Academic, New York, 1972), Vol. 2; Rep. Prog. Phys. **43**, 833 (1980).

[35]T. Takahashi, H. Matsuyama, H. Katayama-Yoshida, Y. Okuabe, S. Hasoya, K. Seki, H. Fukimoto, M. Sato, and H. Inokuchi, Nature **334**, 691 (1988).

[36]Z. X. Shen, P. A. P. Lindberg, P. Soukiassian, C. E. Eom, I. Lindau, W. E. Spicer, and T. H. Geballe, Phys. Rev. B **39**, 823 (1989).

[37]T. Takahashi, H. Matsuyama, H. Katayama-Yoshida, K. Seki, K. Kamiya, and H. Inokuchi, Physica C **170**, 416 (1990).

[38]H. Matsuyama, T. Takahashi, H. Katayama-Yoshida, T. Kashiwakura, Y. Okabe, and S. Sato, Physica C **160**, 567 (1989).

[39]M. S. Golden, S. J. Golden, R. G. Egdell, and W. R. Flavell, in *Proceedings of E-MRS Spring Meeting* (Strasbourg), edited by H.-U. Habermaier and E. Kaldis (Elsevier, Amsterdam, 1990).

[40]G. Mante, Th. Schmalz, R. Manzke, M. Skibowski, M. Alexander, and J. Fink, Surf. Sci. (to be published).

[41]G. Mante, R. Claessen, H. Huss, R. Manzke, M. Skibowski, Th. Wolf, M. Küpfer, and J. Fink, Phys. Rev. B **44**, 9500 (1991).

[42]S. Uchida, H. Takagi, Y. Tokura, N. Koshihara, and T. Arima, in *Strong Correlation and Superconductivity,* edited by H. Fukuyama, S. Maekawa, and A. P. Malozemoff (Springer-Berlin, 1989); S. Uchida, Physica C **185-189**, 28 (1991).

[43]M. Boekholt and G. Güntherodt, Physica C **181**, 179 (1991); M. Boekholt, G. Güntherodt, and V. V. Moshchalkov, Physica C **92**, 191 (1992).

[44]T. Takahashi, S. Suzuki, T. Kusunoki, S. Sato, H.

Katayama-Yoshide, A. Yamanaka, F. Minami, and S. Takekawa, Physica C **185-189**, 1057 (1991).
[45]W. Stephan and P. Horsch, Phys. Rev. Lett. **66**, 2258 (1991).
[46]J. Wagner, W. Hanke, and D. J. Scalapino, Phys. Rev. B **43**, 10 517 (1991).
[47]F. C. Zhang and T. M. Rice, Phys. Rev. B **37**, 3759 (1988).
[48]M. Sasaki, Ishihara, M. Matsumoto, and M. Tachiki, Physica C **185-189**, 1491 (1991).
[49]G. Dopf, A. Muramatsu, and W. Hanke, Phys. Rev. B **41**, 9264 (1990).
[50]P. W. Anderson, Phys. Rev. **109**, 1492 (1958).
[51]V. V. Moshchalkov, Physica C **156**, 473 (1988); Physica B **163**, 59 (1990).
[52]V. V. Moshchalkov, Solid State Commun. **73**, 777 (1990).
[53]E. Abrahams, P. W. Anderson, D. C. Licciardello, and T. V. Ramakrishnan, Phys. Rev. Lett. **42**, 673 (1979).